JOURNAL OF THE MECHANICAL BEHAVIOR OF BIOMEDICAL MATERIALS 51 (2015) 13–24

Available online at www.sciencedirect.com

ScienceDirect

www.elsevier.com/locate/jmbbm

Research Paper

In-vivo degradation of middle-term highly cross-linked and remelted polyethylene cups: Modification induced by creep, wear and oxidation

Yoshihiro Miura[a], *Masahiro Hasegawa*[a,*], *Akihiro Sudo*[a], *Giuseppe Pezzotti*[b], *Leonardo Puppulin*[c]

[a]*Department of Orthopaedic Surgery, Mie University, Graduate School of Medicine, 2-174 Edobashi, Tsu 514-8507, Mie, Japan*
[b]*Ceramic Physics Laboratory, Kyoto Institute of Technology, Sakyo-ku, Matsugasaki, 606-8585 Kyoto, Japan*
[c]*Department of Molecular Cell Physiology, Kyoto Prefectural University of Medicine, Kamigyo-ku Hirokoji Agaru, Kawaramachi-dori, 602-8566 Kyoto, Japan*

ARTICLE INFO

Article history:
Received 24 April 2015
Received in revised form
22 June 2015
Accepted 23 June 2015
Available online 9 July 2015

Keywords:
UHMWPE
Total hip arthroplasty
Retrievals
Raman spectroscopy
FT-IR
Oxidation
Wear
Creep

ABSTRACT

In this study Raman (RS) and Fourier Transform Infrared (FT-IR) spectroscopic techniques were exploited to study 11 retrieved liners made of remelted highly cross-linked polyethylene (HXLPE), with the intent to elucidate their in-vivo mechanical and chemical degradation. The retrievals had different follow-ups, ranging from a few months to 7 years of implantation time and belong to the first generation of highly cross-linked and remelted polyethylene clinically introduced in 1999, but still currently implanted. Raman assessments enabled to discriminate contributes of wear and creep on the total reduction of thickness in different locations of the cup. According to our results, although the most of the viscoelastic deformation occurred during the first year (bedding-in period), it progressed during the steady wear state up to 7 years with much lower but not negligible rate. Overall, the wear rate of this remelted HXLPE liner was low. Preliminary analysis on microtomed sections of the liners after in-vivo and in-vitro accelerated aging (ASTM F2003-02) enabled to obtain a phenomenological correlation between the oxidation index (*OI*) and the amount of orthorhombic phase fraction (α_c), which can be easily non-destructively measured by RS. Profiles of α_c obtained from different locations of the cups were used to judge the oxidative degradation of the 11 retrievals, considering also the ex-vivo time elapsed from the revision surgery to the spectroscopic experiments. Low but measurable level of oxidation was detected in all the short-term retrievals, while in the middle-term samples peaks of *OI* were observed in the subsurface (up to $OI=4.5$), presumably induced by the combined effect of mechanical stress, lipid absorption and prolonged ex-vivo shelf-aging in air.

© 2015 Elsevier Ltd. All rights reserved.

*Corresponding author.
E-mail address: masahase@clin.medic.mie-u.ac.jp (M. Hasegawa).

http://dx.doi.org/10.1016/j.jmbbm.2015.06.028
1751-6161/© 2015 Elsevier Ltd. All rights reserved.

1. Introduction

Balance among wear, creep and oxidation resistance of UHMWPE exposed to biomechanical loads during implantation in the human body. After almost two decades from the development and launch of the first generation of highly cross-linked polyethylene for total hip arthroplasty (THA), this has become the primary issue to be addressed by scientists and engineers in order to achieve higher standards in long-term survivorship of hip joint replacements. The introduction of radiation cross-linking of ultra-high molecular polyethylene (UHMWPE) in the late 1990s indeed represents the major breakthrough in the research and development of orthopedic bearing materials with superior wear and creep resistance (Dumbleton et al., 2006; Gencur et al., 2006; Kurtz et al., 2011). In fact, by increasing the molecular weight through the formation of cross-links between adjacent molecular chains, the ability of the polymer to undergo large deformation is largely decreased. As a matter of fact, excessive deformation caused by the sliding of the harder femoral head on the surface of the polymer may induce molecular orientation along the direction of plastic flow (namely the direction of deformation). High molecular alignment along the primary sliding direction deteriorates the mechanical resistance of the polymer along the other directions and such a "strain-softening" phenomenon lead to the detachment from the surface of micrometric debris (Wang et al., 1997), which may eventually trigger an acute immune response that results in osteolysis and, ultimately, in joint loosening (James et al., 1993; Oparaugo et al., 2001; Zhu et al., 2001). If from one hand wear is a degradation of the material which occurs on the surface, on the other hand, when we deal with polymers, also the inevitable tendency of the bulk material to deform when subjected to load for prolonged time must carefully taken into consideration during the conception phase of bearings. The viscoelastic deformation (i.e., creep) might be deleterious for the correct function of the prosthesis, especially when it manifests in the form of pinch deformation, which changes the sphericity of the cup and induces equatorial contact and degradation of the fluid-film lubrication (Jin et al., 2006; Meding et al., 2013; Ong et al., 2009). In other words, excessive creep might adversely affect the wear resistance and the stability of the joint in the long term. Despite the different physical origin of wear and creep, from a phenomenological point of view, they both manifest themselves with a reduction of cup thickness, whose total extent is routinely measured both in vivo and on cup retrievals, and cumulatively recorded in clinical data. Moreover they are both exacerbated by oxidative degradation, which is progressing with long-term clinical use, leading to debris formation and, ultimately, to joint loosening, or, in the most unfortunate cases, to the premature mechanical failure of the component (Schmalzried and Callaghan, 1999). The first generation of HXLPEs was manufactured with including a melting or annealing step in order to quench the excess of free radicals generated during irradiation, which may eventually react with the oxygen dissolved in the polymer and lead to oxidative degradation (Yeom et al., 1998). However, the results of the first studies on retrievals made of first generation HXLPE showed the unexpected appearance of mechanical and chemical degradation (Currier et al., 2007, 2010). If from one hand a simple post-irradiation annealing step has proved to be insufficient to remove all the free radicals generated during cross-linking (Oral et al., 2011), on the other hand post-irradiation remelting reduces the crystallinity of the final microstructure, which conspicuously decreases the mechanical strength of the polymer (Baker et al., 2003; Gillis et al., 1999; Gomoll et al., 2001; Oral et al., 2011), and can not protect the material from possible generation of free-radicals during in-vivo service. In the attempt to enhance wear and oxidation resistance, a second generation of HXLPEs was engineered by introducing two alternative methods. The first one is based on a 3-step irradiation and annealing process, using a lower dose of γ-ray at each step (i.e., 30 kGy), which enables to optimize the efficiency of the cross-linking during each annealing, to

Table 1 – List of retrievals and their clinical data.

No.	In-vivo time (mo/yr)	Ex-vivo time (mo/yr)	Age (yr)	Sex	BMI (Kg/m^2)	Abd. Angle (°)	Thickness (mm)	Cause of revision	Femoral head
Short term									
No 1	0.5/0.04	137/11.4	71	F	29	45	10.3	Cup loosening	Zirconia
No 2	1.0/0.08	6.0/0.50	58	F	35	46	6.3	Infection	Delta
No 3	1.5/0.13	92/7.70	71	F	18	35	15.4	Infection	Zirconia
No 4	3.0/0.25	74/6.20	67	F	29	39	8.2	Dislocation	Zirconia
No 5	6.0/0.50	39/3.30	78	F	20	30	7.2	Cup loosening	CoCr
No 6	6.5/0.54	94/7.80	71	F	26	40	15.4	Stem loosening	Zirconia
No 7	8.0/0.67	89/7.40	32	M	26	47	12.4	Neuro-paralysis	CoCr
Middle term									
No 8	49/4.10	50/4.20	72	F	33	45	6.4	Dislocation	CoCr
No 9	73/6.10	76/6.30	68	F	30	40	8.2	Stem loosening	Zirconia
No 10	77/6.40	78/6.50	61	F	25	48	7.2	Stem loosening	Zirconia
No 11	86/7.20	15/1.30	75	F	20	45	6.3	Infection	CoCr

preserve high crystallinity and to reduce the number of residual free-radicals, although they are not completely eliminated (Kurtz, 2009). The second one was conceived to strongly counteract the long-term oxidation by incorporating in the resin the antioxidant vitamin E (blended or infused after cross-linking) and to increase fatigue and wear resistance (Bracco and Oral, 2011; Shibata et al., 2006; Teramura et al., 2008). Nevertheless, implantation of acetabular cups which belong to the first generation of HXLPE is still a recurrent procedure in many orthopedic clinics all around the world. In the present paper we show the results of the analyses on 11 retrievals made of the same type of remelted HXLPE (Longevity; Zimmer) with different follow-ups, ranging from a few months to 7 years of implantation time. Several clinical studies on remelted HXLPE have been published during the past decade, which showed interesting data on wear, femoral head penetration and oxidation occurred during in-vivo service (Bragdon et al., 2007; Currier et al., 2007, 2010; Digas et al., 2004; Fukui et al., 2013; Geller et al., 2006; Manning et al., 2005; Muratoglu et al., 2010; Rowell et al., 2014; Thomas et al., 2011), but only a few of them reported follow-ups longer than 4 years (Fukui et al., 2013; Muratoglu et al., 2010; Thomas et al., 2011). We used and implemented an experimental protocol based on Raman (RS) and Fourier transform infrared (FT-IR) spectroscopies which we already introduced in some of our previous papers to systematically study the level of degradation induced by wear, creep and oxidation on the microstructure of polyethylene (Kumakura et al., 2009; Okita et al., 2014; Pezzotti et al., 2007, 2011; Puppulin et al., 2011), with the intent of understanding how these phenomena progress during the implantation time and how they affect each other.

2. Materials and methods

2.1. HXLPE retrievals

A total of 11 retrieved acetabular cups were obtained after periods of time from the respective hip arthroplasty revision surgeries ranging from 0.5 to 11.4 years. Seven cups were short-term in-vivo exposed (between 2 weeks and 8 months) and 4 cups were middle-term in-vivo exposed (between 4.1 and 7.2 years). Table 1 shows the list of the retrievals, which includes the clinical data of the respective patient, the implantation time (hereafter referred as in-vivo time), the shelf-aging time in air elapsed from the revision surgery to the spectroscopic analysis (hereafter referred as ex-vivo time), the cause of revision and the type of femoral head. All the cups were made of the same brand of HXLPE, Longevity (Zimmer, Inc.; Warsaw, Indiana, USA), which belongs to the first-generation remelted polyethylene clinically introduced in the Trilogy acetabular cup design since 1999. The liners were machined from molded sheets, which were previously consolidated from GUR 1050 resin (5.5–6 million g/mol), cross-linked by electron beam with a total dose of 100 kGy at 40 °C and then remelted (>135 °C) to quench residual free radicals.

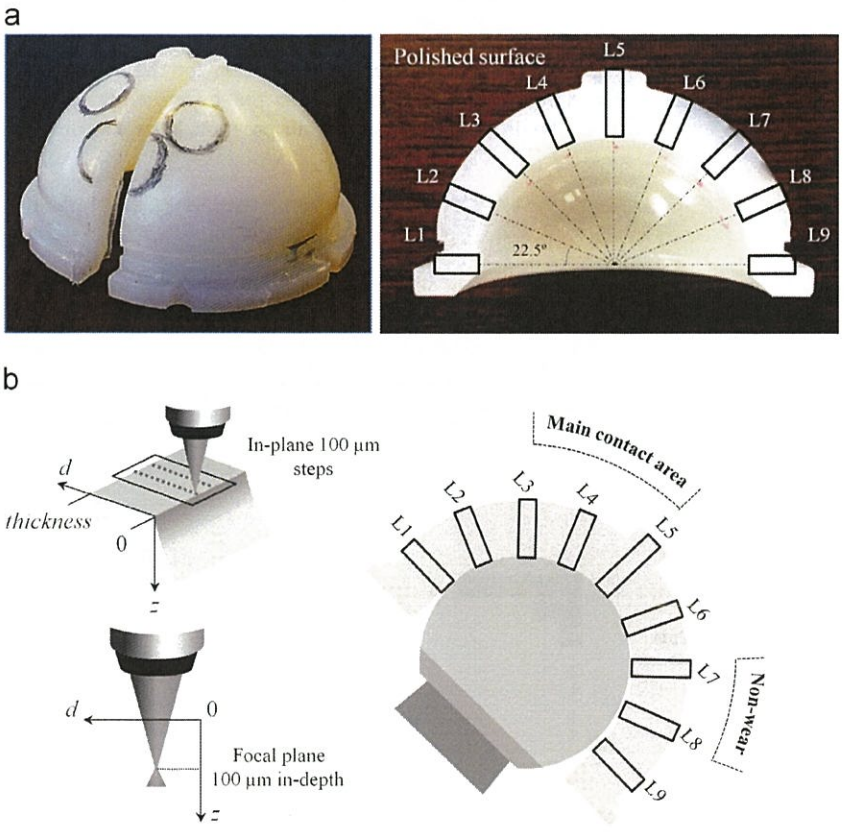

Fig. 1 – (a) Example of retrieved cup sectioned along the meridian line passing through the main contact area. (b) Schematics of the RS protocol used to analyze the in-vivo retrievals at different locations (L1–L9).

The final sterilization of the acetabular component was made by gas plasma after packaging in a gas-permeable pouch. All the retrievals were cut along the meridian line of the cup intercepting the wear zone in order perform line scans of Raman spectra along the thickness. The surface after cut was carefully polished and spectra were collected at 100 μm in-depth to neglect possible microstructural modifications induced by cutting. In Fig. 1 are shown explicative sketches of the cup sectioning, the investigated locations of each liner and the protocol of spectra acquisition.

2.2. *In-vitro and in-vivo oxidized HXLPE sections*

Preliminary study by FT-IR and RS of in-vitro and in-vivo oxidized samples enabled to find a phenomenological correlation between oxidation index (*OI*) and orthorhombic phase fraction of the HXLPE under investigation. One new Longevity cup was cut through its thickness to obtain a rectangular prism from the bottom of the cup. The prism was cut in half and 200 μm sections were microtomed. One slice was immediately analyzed by IR and RS to characterize the acetabular cup as received. For the rest of the slices, the accelerated aging test was performed according to the standards ASTM F2003-02 (reapproved in 2008) (Standard, 2008). The slices underwent to a preliminary conditioning step which consisted of irradiating the specimens with γ-ray (25 kGy dose) and maintaining them at 23 °C for 28 days. Subsequently, the spectroscopic analyses were conducted on one slice, while the remnant was placed in an oxygen bomb at 70 °C under 5 atm. of pure oxygen for 3, 14, and 28 days. The aging test on irradiated slices was performed with the aim of characterizing the microstructural modifications in a wide range of *OI*. In addition, FT-IR and RS analyses were performed on a microtomed section obtained from one of the retrievals (sample no. 8). Extraction of lipids and contaminants was achieved by soaking the slice in boiling hexanes (69 °C) for 18 h. Fig. 2(a) shows pictures of some of the in-vitro and in-vivo oxidized HXLPE sections.

2.3. *Raman spectroscopy*

Raman microprobe spectrometer (T-64000, Horiba/ Jobin-Yvon, Kyoto, Japan) in back-scattering geometry was used to characterize the microstructures of the oxidized polyethylene slices and the retrievals. The excitation source was a 532 nm diode laser (SOC Juno, Showa Optronics Co., Ltd, Tokyo, Japan) yielding a power of approximately 9 mW on the UHMWPE liner surface. The recorded non-polarized spectra were averaged over three successive measurements at each selected location. A spectral resolution better than 0.15 cm^{-1} was achieved by means of an 1800 l/mm grating. Spectral deconvolution has been performed by means of an automatic fitting algorithm enclosed in a commercially available computational package (Labspec 5, Horiba/Jobin-Yvon, Kyoto, Japan), using mixed Gaussian/Lorentzian curves. The relationship between the observed Raman bands and the vibrational modes of the polyethylene molecular structure has been amply documented in the literature (Glotin and Mandelkern, 1982; Mutter et al., 1993; Naylor et al., 1995; Rull et al., 1993; Strobl and Hagedorn, 1978). The reduction of liner thickness due to wear and creep was assessed using the width of the Raman band located at 1130 cm^{-1} (A_g+B_{1g} mode or symmetric stretching of C–C bonds) as a sensor for residual strain in the polymeric network because it reflects the degree of disorder of the polymeric network, which is directly affected by strain. Calibration experiments of band broadening as a function of residual compressive strain for the Longevity HXLPE were conducted according to the experimental protocol already reported in some of our previous papers (Okita et al., 2014; Pezzotti et al.,

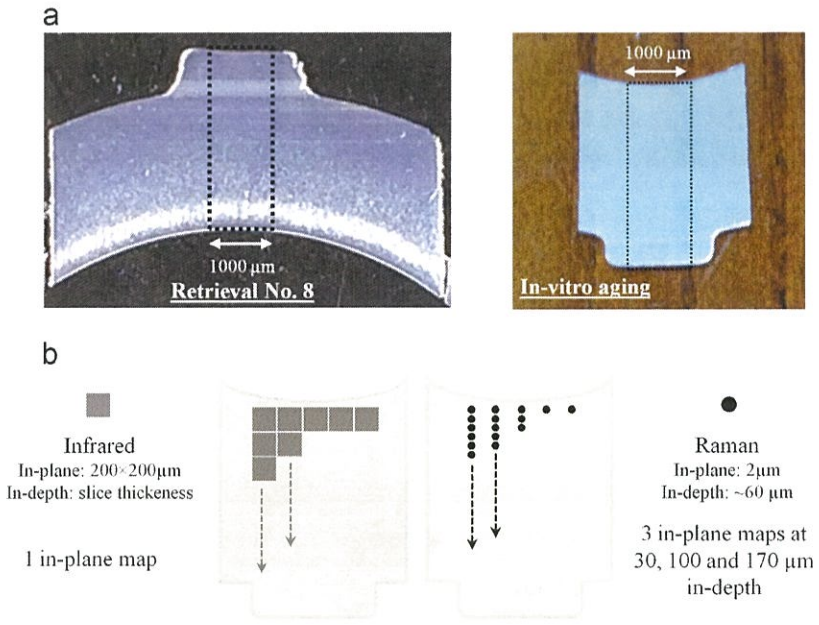

Fig. 2 – Thin section obtained from Retrieval No.8 (L5) and from a new cup for accelerated aging. The retrieved sample presents a clear white stripe at 1 mm in-depth from the sliding surface, due to heavy oxidation. (b) Schematics of the spectroscopic protocol used to analyze the oxidized UHMWPE sections.

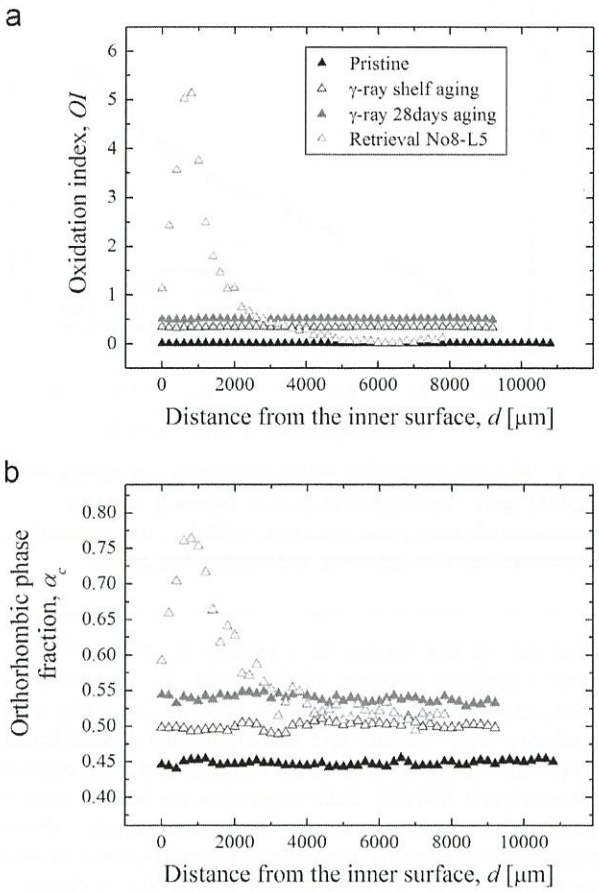

Fig. 3 – (a) *In-depth* profiles of *OI* calculated from the sections of pristine, γ-irradiated/shelf aged, γ-irradiated/28-day aged and in-vivo oxidized materials calculated by FT-IR. (b) Similarly, crystalline phase profiles calculated from the RS analysis of the same samples as in (a).

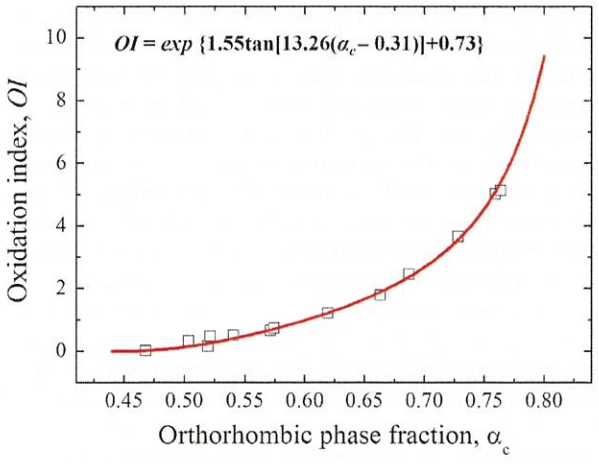

Fig. 4 – Phenomenological correlation between crystalline phase fraction and *OI* as obtained from the experimental results shown in Fig. 3.

2011; Puppulin et al., 2014), which enabled us to obtain the phenomenological equation to quantify the percentage of creep along the thickness of the retrievals. The regression analysis was performed using Origin Pro 8.5 (OriginLab, Northampton, MA) and Minitab 17 Statistical Software (State College, PA: Minitab, Inc.). For each retrieval, at different 9 polar locations (see. Fig. 1, hereafter referred to as L1-L9), Raman spectra were collected along the thickness (*d* abscissa), with step of 100 μm, from the inner to the outer surface of the liner. For each polar location, the in-depth creep profiles were calculated from the average of two line scans. Strain data at each polar location were translated into thickness variations due to creep (Δt_c) by integrating the in-depth strain profile over the in-depth abscissa through the entire thickness of the polyethylene liner. The thickness variation due to wear (Δt_w) was then calculated by subtracting Δt_c to the total reduction of thickness calculated by standard methods based on micrometric motorized stage coupled with optical microscope. As far as the investigation of oxidized thin sections is concerned, RS was used to calculate profiles of orthorhombic crystalline phase fraction (α_c) from the inner to the outer surface of the cup. Phenomenological correlation between α_c and *OI* was obtained by comparing RS and FT-IR data (see next paragraph 2.4). While the transmission infrared spectroscopy has an in-plane spatial resolution of 200 × 200 μm^2 and the whole thickness of the section is probed by the infrared beam, Raman probe is confined in tens of microns around the focal plane. The configuration of the probe adopted throughout the analysis of the oxidized sections corresponded to a 100 × objective and a pinhole diameter fixed at Φ=1 mm, giving an in-depth probe size of ~60 μm (Pezzotti et al., 2007). In Fig. 2(b) the mapping procedure followed in the RS experiments is schematically explained in comparison to the FT-IR sampling procedure. Raman maps on the sections were collected at 3 different depths in order to characterize the entire thickness and to statistically correlate the results retrieved on the same sample using two different experimental techniques.

In the case of α_c assessments, we used the method introduced by Strobl and Hagerdon, which is based on a set of equations that includes the intensities of vibrational bands located at 1296, 1305 and 1418 cm^{-1}, as obtained from unpolarized Raman spectra (Strobl and Hagedorn, 1978). In detail, the fraction of orthorhombic crystalline (α_c) can be calculated from the Raman spectrum of polyethylene, according to the following equation:

$$\alpha_c = \frac{I_{1414}}{0.46(I_{1293} + I_{1305})} \quad (1)$$

where *I* is the integral intensity of each individual Raman band identified by the subscript (i.e., after spectral deconvolution). From the spectra collected at different polar locations of the retrievals for creep analysis we also obtained profiles of α_c, which were converted to profile of *OI* by means of the phenomenological equation.

2.4. *Fourier transform infrared spectroscopy*

Oxidation profiles of microtomed sections were determined using FT-IR as a function of depth away from the inner surface of the cup. FT-IR microscopic analysis was carried out using the imaging system Spotlight 200 (Perkin Elmer, Waltham, Massachusetts, USA). Infrared transmission spectra of polyethylene were acquired at aperture size of 200 × 200 μm^2. An *OI* was calculated according to ASTM 2102 as the ratio of the area under

the carbonyl peak at around 1720 cm^{-1} to the area under the C–H absorption peak centered around 1370 cm^{-1} (Standard, 2006). In order to create oxidation profiles as a function of depth, the adopted experimental routine was conceived as follows: five line scans were collected from the sliding surface to the back-surface of the liner with 200 μm steps. The *OI* at each depth was calculated as the average of 5 measurements. The investigated area was the same previously analyzed by RS (see Fig. 2(b))

3. Results

3.1. *In-vitro and in-vivo oxidized slices*

FT-IR analysis and Raman maps collected at different depths from the polyethylene slices after accelerated aging test visualized the evolution of *OI* and crystalline phase content during oxidation. Profiles of *OI* are shown in Fig. 3(a) as calculated from FT-IR spectra collected from the slices of the pristine, the 28 days shelf-aged material after irradiation, the 28 days irradiated and in-vitro aged material and the retrieval no. 8 (location L5). The pristine showed very low amount of oxidized species, with *OI* equal to 0 in the most of the analyzed locations and a peak of 0.01. The oxidative degradation of the polymer in the samples after in-vitro aging clearly increased with the time and it was also homogeneous throughout the thickness of the cup. Different outcomes were obtained from the FT-IR analysis of the middle-term retrieval. This slice was microtomed from the location 5 of the cup, which belongs to the main contact area with the femoral head. The onset of a high peak of oxidation was observed around 1 mm in-depth from the sliding surface of the bearing, which was somewhat unexpected considering the magnitude of detected *OI* equal to 5.1. Similarly to infrared analysis, profiles of α_c were obtained from the RS investigation of the same slices, whose results are shown in Fig. 3(b). For each slice, the similarity between the trends of crystallinity and *OI* along the thickness was evident. Fig. 4 shows the phenomenological correlation between α_c and *OI* as obtained upon plotting the experimental data collected from all the slices. The data in the plot represent the average α_c and *OI* calculated from points with similar *OI* (i.e., variation of 0.1 was set as significant). Correlations between crystallinity and *OI* could be obtained by fitting the experimental data with an exponential function that we already introduced in a previous study (Pezzotti et al., 2007). According to the partial-least-square fitting method, the following equations could be obtained for the Longevity material:

$$OI = e^{\{1.25 \tan(6.38\alpha_c - 4.23) + 0.69\}} \quad (2)$$

with coefficient of correlation, adjusted-R^2, equal to 0.98. This equation was used to assess the degree of oxidation in different locations of the 11 retrievals by means of RS.

3.2. *Correlation between creep and Raman band broadening*

According to the experimental procedures described in some of our previous papers (Okita et al., 2014; Pezzotti et al., 2011; Puppulin et al., 2014), samples made of Longevity remelted HXLPE were analyzed to obtain the phenomenological correlation between compressive residual strain after recovery and broadening of the Raman band located at 1130 cm^{-1} (symmetric stretching vibration of C–C bond). Fig. 5 shows the correlation between the percentage compressive strain measured after 24 h recovery and the experimental band broadening, which was measured as the variation of the full width at half maximum (FWHM). Cubic regression model was used to calculate the best-fitting curve (cf. best-fitting equation shown in the inset) and the confidance bands (confidence level of 95%). The standard error of the regression (*S*) and the coefficient of correlation (R^2) were 0.25% and 0.996, respectively.

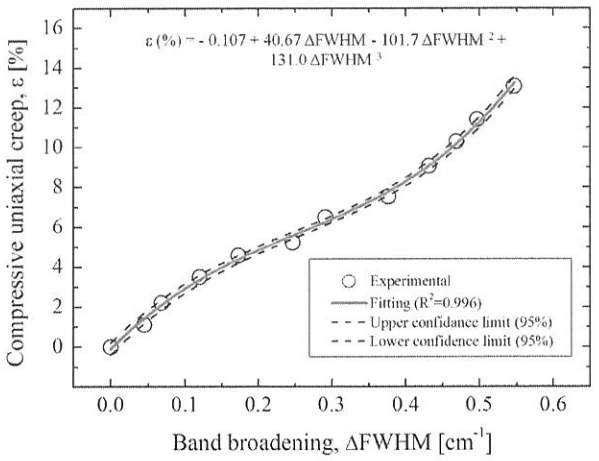

Fig. 5 – Phenomenological correlation between compressive residual strain measured after 24 h recovery and the experimental band broadening (ΔFWHM). Cubic regression model was used to calculate the best-fitting curve.

3.3. *Wear, creep and oxidation of retrievals*

Fig. 6 shows the results of creep, wear and total penetration as calculated from the short term retrievals using the method based on RS. For each cup, the data were plotted in polar coordinates according to the angle of each of the 9 locations in which the thickness were measured by micro-metric motorized stage combined with optical microscope and analyzed by RS. The profiles were obtained by B-spline interpolation of the experimental points. The polynomial fitting equation used to assess the percentage of creep deformation has an error of 0.5% (i.e., 2S, 95% confidence level). In all the seven short-term retrievals the reductions of thickness due to wear as obtained by subtracting creep to the total penetration gave positive or negative values of few tens of microns, which were comparable to the error integrated over the entire thickness. In fact, an error of 0.5% in strain assessment integrated over the maximum thickness of 15.4 mm yields a maximum error of 77 μm, while for the 6.3 mm cups the maximum error is estimated at 31.5 μm. For this reason, the wear in the short-term cups was neglected and the total creep was considered as equal to the total penetration. It was clear that sample No.1 and 2 had the lowest residual strain among the short-term retrievals, mainly localized between L3 and L6, while the cups with follow-up longer than 6 months (No.6 and 7) showed peaks of penetration higher than 100 μm and detectable deformation

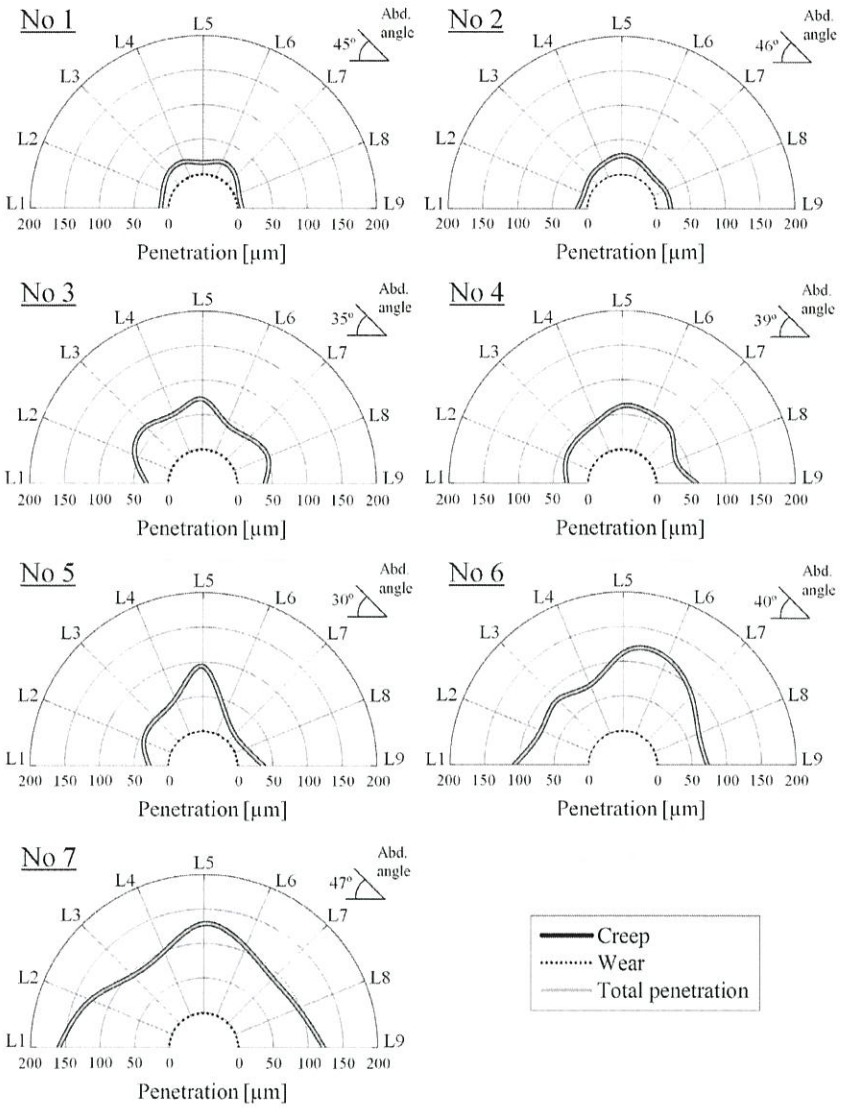

Fig. 6 – Polar graphs representing profiles of creep, wear and total penetration as interpolated from the data of the short-term retrievals.

also near the rim, presumably due to stem impingement and heel strike. The highest deformation near the rim (L1 and L9) was detected in sample No. 7, which had the longest follow-up and high abduction angle (47°), which favors the impingement of the neck of the stem against the rim and heel strike. In sample No. 5 the deformation was localized around the top of the cup (L5), which might be correlated to the low abduction angle (30°). Similarly to Fig. 6, the results of the four middle-term retrievals are reported in the polar plots of Fig. 7. The onset of wear clearly showed up in all the middle-term liners, manly localized between L3 and L6, with the exception of liner no. 9, in which the reduction of thickness was lower in magnitude but widespread between L1 and L6, probably due to the low abduction angle (40°). Sample No. 8 was characterized by the highest creep and the wear damage was sharply localized in L4, as expected by the abduction angle of 45°. Interestingly, the patient of the latter retrieval had the highest BMI among the four (BMI=33) and suffered dislocation, which might explain the magnitude of residual strain calculated also in locations that are not supposed to be loaded. Moreover, all the middle-term retrievals showed significant creep deformation in both locations near the rim. The maximum creep, wear and total penetrations calculated from each retrieval as a function of implantation time were plotted in Fig. 8(a)–(c). The linear regression analysis of these data enabled to calculate the creep, wear and total penetration rates during the bedding-in period, the steady wear state period and the overall range of follow-ups. The results are reported in Table 2, in which are also included the respective Pearson's correlation index (r). According to Eq. (2), RS analysis enabled to study the oxidative degradation of the retrievals at different locations. Peak of OI as well as average OI calculated in the wear (L3–L5) and nonwear zone (L7, L8) are shown in Fig. 9(a) and (b) for the short and middle-term retrievals, respectively. In the short-term retrievals the peak of oxidation are similar (OI ~0.2), while the average

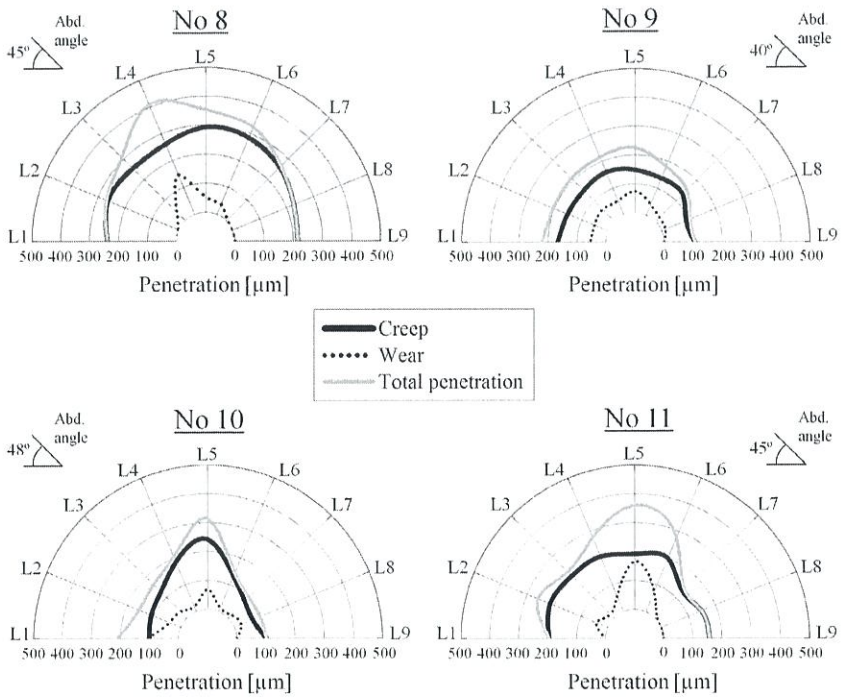

Fig. 7 – Similarly to Fig. 6, polar graphs representing profiles of creep, wear and total penetration obtained from the middle-term retrievals.

oxidation in the wear and non-wear zones was very low. Interestingly, the lowest mean oxidation was detected in sample No. 2, which had the shortest ex-vivo time. In the middle-term retrievals the peaks of *OI* were detected under the worn area and they ranged from 1.4 to 4.5. Moreover, in samples No. 8 and 9 the average oxidation of the wear zone was higher than that calculated from the non-wear zone, which might suggest some influence of the mechanical load on the oxidation of polyethylene.

4. Discussion

The oxidative degradation of remelted HXLPE was studied by analyzing in-vitro aged samples microtomed from new liners. As shown in Fig. 3, the in-depth profiles of oxidation clearly shifted toward higher values of *OI* after shelf- and accelerated aging, although their shape did not change. If we consider that the distribution of free radicals generated by the preliminary step of gamma irradiation was uniform throughout the intere slices, we can infer that there were no gradients of residual free radicals along the thickness of the virgin liners. The major increase of *OI* (from 0 to around 0.4) occurred within the 28 days of shelf-aging in air after irradiation, while during accelerated aging at 70 °C all the few residual free-radicals recombined with oxygen leading to the maximum *OI* of 0.51. For each slice, the similarity between the trends of crystallinity and *OI* along the thickness was evident and it highlighted the recrystallization process triggered by the formation of oxidized species. In fact, if free radicals are formed inside the amorphous phase of polyethylene, they react with oxygen leading to the formation of hydroperoxides (i.e., first product of oxidation) (Bracco et al., 2006a, 2006b; Costa et al., 1997). Hydroperoxides can evolve to ketones, carboxyl acids and other oxidized species containing carbonyl groups, whose formation is responsible for the polyethylene chain breakage, namely chain shortening, increase of molecular mobility and subsequent recrystallization. Comparison among slices at different oxidative conditions showed that major recrystallization rate occurred at the early stage of oxidation, up to *OI* of about 0.4. The results showed in Fig. 4 confirmed that the equation introduced in our previous studies is suitable in describing the oxidation-induced recrystallization process of different polyethylenes.

Raman spectroscopy offered the possibility to scrutinize in an accurate and nimble way the microstructures of 11 retrievals made of first generation remelted HXLPE. The samples were divided in two groups, according to the implantation time: 7 short term cups with less than 1 year follow-up and 4 middle term cups (from 4 to 7 years). The fast acquisition time and the motorized stage of the spectrophotometer enabled us to characterize the material collecting a number of Raman spectra which represents a statistically meaningful sample size. Overall, the creep deformation in the seven short-term retrievals was very low but constantly increasing with the implantation time. Interestingly, the only short-term retrieval with implantation time close to 1 year (No. 7) showed creep deformation which was not significantly lower than those calculated from the middle term retrievals, confirming that after the initial bedding-in period the head penetration rate due to plastic deformation is low (Geller et al., 2006; Laurent et al., 2008; Manning et al., 2005), but it should be considered in the case-by-case analysis. This argument is strengthened by considering the data of Fig. 8 (a)–(c) and Table 2. Wear rate during the steady state was

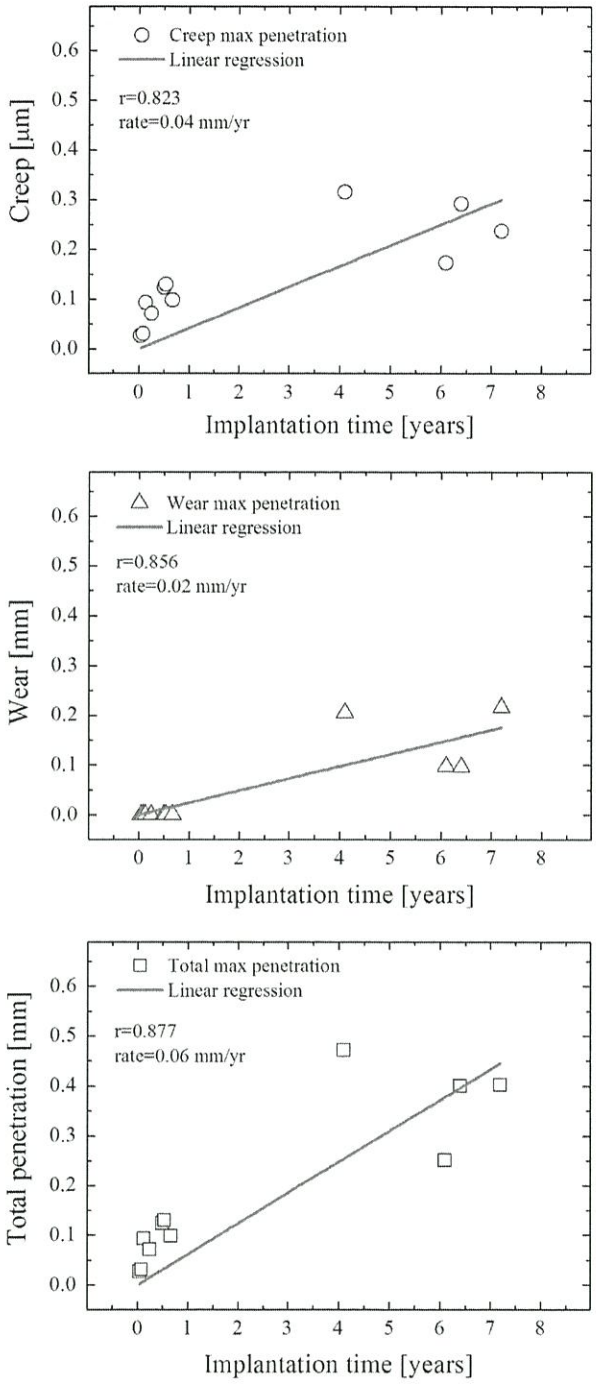

Fig. 8 – Peaks of creep (a), wear (b) and total penetration (c) as a function of implantation time. Linear regression lines were calculated considering the bedding-in period, the steady wear state period and the overall range of follow-ups.

0.020 mm/y, which was low but comparable to the amount of creep deformation. In fact, the plastic deformation experienced after bedding-in period was 0.010 mm/y, although r was low, due to the scattered distribution of the 4 middle-term data, and the rate consistently dropped down from 0.189 mm/y experienced during bedding-in. Sample no.8 had the highest peak of creep deformation among the four retrievals and the shortest implantation time, while sample no. 9 had creep comparable to the 8-month retrieval no. 7. Interestingly, the retrievals no. 8 and 11 showed the highest peaks of wear and they were both coupled with CoCr femoral head, while the other two middle-term retrievals (No. 9 and 10) were implanted with Zirconia femoral heads. Considering the regression lines of the overall data, wear and creep rates were equal (0.026 mm/y). The total penetration rates were 0.189 mm/y, 0.027 mm/y and 0.046 mm/y for the bedding in, steady wear and overall periods, respectively. These latter data must be considered for comparison with previous clinical studies on remelted HXLPE published in the past. In fact, all the methods used in these studies are not capable of discriminating between the amount of femoral head penetration due to wear damage or creep, but they only rely on the consideration that during the initial bedding in period the thickness variation should be related to plastic deformation, while during the successive period of implantation the penetration should be associated to wear (i.e., steady-state wear). Manning et al. reported results of retrievals at maximal 44-month follow-up, which were obtained by radiographies and showed an overall penetration rate of 0.018 mm/y, with a peak of 0.4 mm/y registered after 6 months and a steady-state wear estimated to be 0.07 mm/y (Manning et al., 2005). Also Geller et al., 2006 presented a clinical study of Longevity retrievals based on radiographic evaluation of femoral head penetration (36 and 40-mm heads) in 71 patients. The median penetration during the first postoperative year was 0.24 mm, due to creep (bedding in period), while up to 3 years of implantation the median steady wear rate dropped down to 0.06 mm/y (Geller et al., 2006). In a different study, the same authors used radiostereometric analysis to measure the femoral head penetration in retrievals of 28 and 36-mm head size, reporting the highest penetration rate during the first year of implantation of 0.055 mm/y, while during the second and third year there was no significant variation of head penetration indicating no occurrence of wear damage (Bragdon et al., 2007). In-vitro wear simulations conducted on Longevity liners showed much lower wear rates than those measured after explantation (Laurent et al., 2008), confirming the necessity of conducting more clinical studies on retrievals to fully understand the response of the polymeric microstructure once exposed to in-vivo conditions.

As far as the analysis of oxidation is concerned, Muratoglu et al. reported no detectable oxidation in remelted HXLPE cups after explantation, but, conversely, they strikingly underwent to heavy oxidation after ex-vivo shelf-aging in air (Muratoglu et al., 2010), which was the same case of our retrievals. Oral et al. proposed a new mechanism of oxidation in UHMWPE caused by lipids absorption, which are present in the synovial fluid and during implantation might trigger accelerated oxidation and degradation of the mechanical properties of these materials (Oral et al., 2012). The oxidation rate should be dependent on lipid concentration, oxygen concentration, time and temperature. A limitation of this investigation is certainly the fact that we could not analyze the samples immediately after explantation, which made impossible to discriminate between in-vivo and ex-vivo oxidation. Nevertheless, some interesting conclusions could be drawn considering the differences among the ex-vivo

Table 2 – Creep, wear and total penetration rates [mm/yr] as calculated from the fitting of the plots in Fig. 8.

	Bedding-in		Steady wear state		Overall	
	Rate	r	Rate	r	Rate	r
Creep	0.189	0.946	0.010	0.375	0.026	0.798
Wear	0.000	0.000	0.022	0.634	0.026	0.857
Total penetration	0.189	0.946	0.027	0.534	0.046	0.849

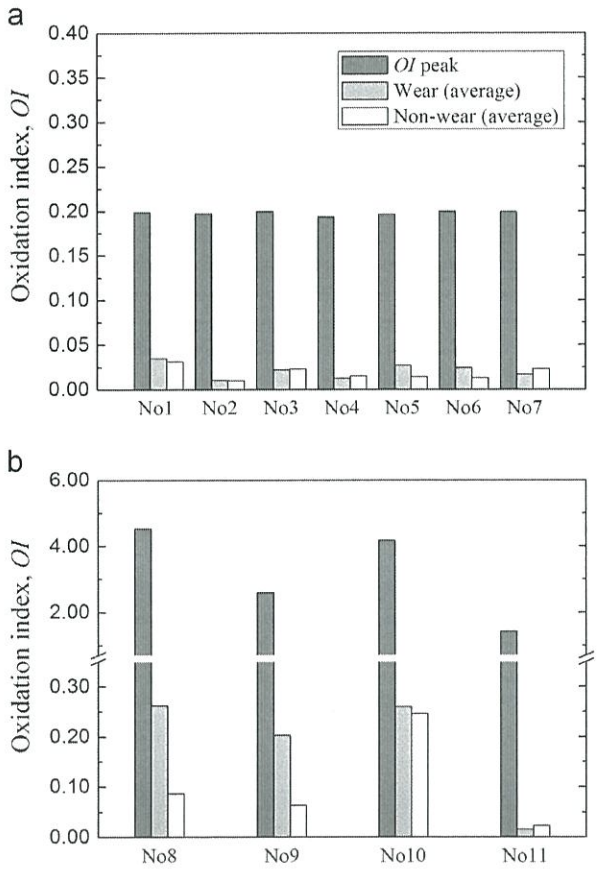

Fig. 9 – Peak of *OI*, average *OI* in the wear zone (L3-L5) and non-wear zone (L7, L8) for the short-term (a) and middle-term (b) retrievals, respectively.

times and the peaks of oxidation located under the worn surfaces. In fact, the shortest ex-vivo time was 6 months for the sample no. 2, but it was sufficient to induce the same maximum level of oxidation (i.e., $OI \sim 0.2$) obtained from the other short term retrievals, although the means calculated from the wear and nonwear zone are slightly lower, which might confirm that oxidation was proceeding ex-vivo (see Fig. 9(a)). Interestingly, the peaks of *OI* largely increased in the middle-term retrievals and were detected in the subsurface of the main contact area (see also the *OI* profile of Fig. 3(a) and the clear white stripe in Fig. 2(a) at around 1 mm in-depth from the sliding surface of sample No. 8), but the average values in the wear and nonwear zone did not increase at the same extent. This experimental evidence might indicate that the formation of free radicals is favored by the mechanical load of the femoral head, which promote lipid diffusion and the rupture of the C–C bonds, especially beneath the surface where the highest contact stress is predicted by the Hertzian equation, localized at 1 mm in-depth in our retrievals. Although Sample No. 11 spent the longest implantation time, it showed less oxidative degradation as compared to the other middle-term retrievals, probably due to the shortest ex-vivo time. In conclusion, these latter results showed that remelted HXLPE might be affected by long-term oxidation when exposed to the biological environment of the human body and that the oxidative degradation depends on the lipid concentration, the time and it is assisted by mechanical stress. If from one hand the results of the present study give new insight into the in-vivo performance of remelted HXLPE, on the other hand it is clear that the number of analyzed samples is a limitation, especially in the case of the middle-term explants ($n=4$), which implies that further clinical studies are mandatory to confirm these outcomes.

5. Conclusion

The preliminary study on samples after in-vivo and in-vitro aging enabled to unfold the microstructural modifications induced by the oxidative degradation in the remelted HXLPE and to obtain a phenomenological equation to calculate *OI* from the data of α_c collected by RS. Based on the Raman spectroscopic protocol of analysis, 11 retrievals made of highly cross-linked and remelted polyethylene were systematically scrutinized to calculate the degree of creep, wear and oxidation at different location of the cups. As expected, the most of the creep penetration occurred during the bedding-in period, but it progressed also after the first year, with low rates but not negligible as compared to the wear penetration rate. Wear of this highly cross-linked material was very low, which confirmed previous studies with lower or similar follow-ups. Oxidation was detected, probably mainly occurred during the ex-vivo time, but certainly correlated to the in-vivo exposure, namely the combined effect of chemical and mechanical degradation, with peaks of *OI* at 1 mm in-depth in all the middle-term retrievals, in which stress and lipids concentration might have encountered the most deleterious combination.

REFERENCES

Baker, D., Bellare, A., Pruitt, L., 2003. The effects of degree of crosslinking on the fatigue crack initiation and propagation resistance of orthopedic-grade polyethylene. J. Biomed. Mater. Res. A 66, 146–154.

Bracco, P., Brunella, V., Luda, M., del Prever, E.B., Zanetti, M., Costa, L., 2006a. Oxidation behaviour in prosthetic UHMWPE components sterilised with high-energy radiation in the presence of oxygen. Polym. Degrad. Stab. 91, 3057–3064.

Bracco, P., Del Prever, E.B., Cannas, M., Luda, M., Costa, L., 2006b. Oxidation behaviour in prosthetic UHMWPE components sterilised with high energy radiation in a low-oxygen environment. Polym. Degrad. Stab. 91, 2030–2038.

Bracco, P., Oral, E., 2011. Vitamin E-stabilized UHMWPE for total joint implants: a review. Clin. Orthop. Relat. Res. 469, 2286–2293.

Bragdon, C.R., Greene, M.E., Freiberg, A.A., Harris, W.H., Malchau, H., 2007. Radiostereometric analysis comparison of wear of highly cross-linked polyethylene against 36-vs 28-mm femoral heads. J. Arthroplasty 22, 125–129.

Costa, L., Luda, M., Trossarelli, L., 1997. Ultra high molecular weight polyethylene—II. Thermal-and photo-oxidation. Polym. Degrad. Stab. 58, 41–54.

Currier, B., Van Citters, D., Currier, J., Collier, J., 2010. In vivo oxidation in remelted highly cross-linked retrievals. J. Bone Jt. Surg. 92, 2409–2418.

Currier, B.H., Currier, J.H., Mayor, M.B., Lyford, K.A., Collier, J.P., Van Citters, D.W., 2007. Evaluation of oxidation and fatigue damage of retrieved crossfire polyethylene acetabular cups. J. Bone Jt. Surg. 89, 2023–2029.

Digas, G., Kärrholm, J., Thanner, J., Malchau, H., Herberts, P., 2004. THE OTTO AUFRANC AWARD: highly cross-linked polyethylene in total hip arthroplasty: randomized evaluation of penetration rate in cemented and uncemented sockets using radiostereometric analysis. Clin. Orthop. Relat. Res. 429, 6–16.

Dumbleton, J.H., D'Antonio, J.A., Manley, M.T., Capello, W.N., Wang, A., 2006. The basis for a second-generation highly cross-linked UHMWPE. Clin. Orthop. Relat. Res. 453, 265–271.

Fukui, K., Kaneuji, A., Sugimori, T., Ichiseki, T., Matsumoto, T., 2013. Wear comparison between conventional and highly cross-linked polyethylene against a zirconia head: a concise follow-up, at an average 10 years, of a previous report. J. Arthroplast. 28, 1654–1658.

Geller, J.A., Malchau, H., Bragdon, C., Greene, M., Harris, W.H., Freiberg, A.A., 2006. Large diameter femoral heads on highly cross-linked polyethylene: minimum 3-year results. Clin. Orthop. Relat. Res. 447, 53–59.

Gencur, S.J., Rimnac, C.M., Kurtz, S.M., 2006. Fatigue crack propagation resistance of virgin and highly crosslinked, thermally treated ultra-high molecular weight polyethylene. Biomaterials 27, 1550–1557.

Gillis, A., Schmieg, J., Bhattacharyya, S., Li, S., 1999. An independent evaluation of the mechanical, chemical and fracture properties of UHMWPE cross linked by 34 different conditions. In: Proceedings of the Annual meeting-Society for biomaterials in conjunction with the international biomaterials symposium, pp. 216–216.

Glotin, M., Mandelkern, L., 1982. A Raman spectroscopic study of the morphological structure of the polyethylenes. Colloid and Polymer Science 260, 182–192.

Gomoll, A., Wanich, T., Bellare, A., 2001. Quantitative measurement of the morphology and fracture toughness of radiation crosslinked UHMWPE. ORS. February.

James, S., Blazka, S., Merrill, E., Jasty, M., Lee, K., Bragdon, C., Harris, W., 1993. Challenge to the concept that UHMWPE acetabular components oxidize in vivo. Biomaterials 14, 643–647.

Jin, Z., Meakins, S., Morlock, M., Parsons, P., Hardaker, C., Flett, M., Isaac, G., 2006. Deformation of press-fitted metallic resurfacing cups. Part 1: experimental simulation. Proc. Inst. Mech. Eng. H 220, 299–309.

Kumakura, T., Puppulin, L., Yamamoto, K., Takahashi, Y., Pezzotti, G., 2009. In-depth oxidation and strain profiles in UHMWPE acetabular cups non-destructively studied by confocal Raman microprobe spectroscopy. J. Biomater. Sci.. Polym. Ed. 20, 1809–1822.

Kurtz, S.M., 2009. Compendium of highly crosslinked UHMWPEs. In: UHMWPE Biomaterials Handbook. Amsterdam.Elsevier, pp. 291–308.

Kurtz, S.M., Gawel, H.A., Patel, J.D., 2011. History and systematic review of wear and osteolysis outcomes for first-generation highly crosslinked polyethylene. Clin. Orthop. Relat. Res. 469, 2262–2277.

Laurent, M.P., Johnson, T.S., Crowninshield, R.D., Blanchard, C.R., Bhambri, S.K., Yao, J.Q., 2008. Characterization of a highly cross-linked ultrahigh molecular-weight polyethylene in clinical use in total hip arthroplasty. J. Arthroplast. 23, 751–761.

Manning, D.W., Chiang, P., Martell, J., Galante, J., Harris, W., 2005. In vivo comparative wear study of traditional and highly cross-linked polyethylene in total hip arthroplasty. J. Arthroplast. 20, 880–886.

Meding, J.B., Small, S.R., Jones, M.E., Berend, M.E., Ritter, M.A., 2013. Acetabular cup design influences deformational response in total hip arthroplasty. Clin. Orthop. Relat. Res. 471, 403–409.

Muratoglu, O.K., Wannomae, K.K., Rowell, S.L., Micheli, B.R., Malchau, H., 2010. Ex vivo stability loss of irradiated and melted ultra-high molecular weight polyethylene. J. Bone Jt. Surg. 92, 2809–2816.

Mutter, R., Stille, W., Strobl, G., 1993. Transition regions and surface melting in partially crystalline polyethylene: a Raman spectroscopic study. J. Polym. Sci. B: Polym. Phys. 31, 99–105.

Naylor, C.C., Meier, R.J., Kip, B.J., Williams, K.P., Mason, S.M., Conroy, N., Gerrard, D.L., 1995. Raman spectroscopy employed for the determination of the intermediate phase in polyethylene. Macromolecules 28, 2969–2978.

Okita, S., Hasegawa, M., Takahashi, Y., Puppulin, L., Sudo, A., Pezzotti, G., 2014. Failure analysis of sandwich-type ceramic-on-ceramic hip joints: a spectroscopic investigation into the role of the polyethylene shell component. J. Mech. Behav. Biomed. Mater. 31, 55–67.

Ong, K.L., Rundell, S., Liepins, I., Laurent, R., Markel, D., Kurtz, S. M., 2009. Biomechanical modeling of acetabular component polyethylene stresses, fracture risk, and wear rate following press-fit implantation. J. Orthop. Res. 27, 1467–1472.

Oparaugo, P.C., Clarke, I.C., Malchau, H., Herberts, P., 2001. Correlation of wear debris-induced osteolysis and revision with volumetric wear-rates of polyethylene: a survey of 8 reports in the literature. Acta Orthop. 72, 22–28.

Oral, E., Ghali, B.W., Muratoglu, O.K., 2011. The elimination of free radicals in irradiated UHMWPEs with and without vitamin E stabilization by annealing under pressure. J. Biomed. Mater. Res. B: Appl. Biomater. 97, 167–174.

Oral, E., Ghali, B.W., Neils, A., Muratoglu, O.K., 2012. A new mechanism of oxidation in ultrahigh molecular weight polyethylene caused by squalene absorption. J. Biomed. Mater. Res. B: Appl. Biomater. 100, 742–751.

Pezzotti, G., Kumakura, T., Yamada, K., Tateiwa, T., Puppulin, L., Zhu, W., Yamamoto, K., 2007. Confocal Raman spectroscopic analysis of cross-linked ultra-high molecular weight polyethylene for application in artificial hip joints. J. Biomed. Opt. 12, 014011–014014.

Pezzotti, G., Takahashi, Y., Takamatsu, S., Puppulin, L., Nishii, T., Miki, H., Sugano, N., 2011. Non-destructively differentiating the roles of creep, wear and oxidation in long-term in vivo exposed polyethylene cups. J. Biomater. Sci. Polym. Ed. 22, 2165–2184.

Puppulin, L., Kumakura, T., Yamamoto, K., Pezzotti, G., 2011. Structural profile of ultra-high molecular weight polyethylene in acetabular cups worn on hip simulators characterized by confocal Raman spectroscopy. J. Orthop. Res. 29, 893–899.

Puppulin, L., Sugano, N., Zhu, W., Pezzotti, G., 2014. Structural modifications induced by compressive plastic deformation in single-step and sequentially irradiated UHMWPE for hip joint components. J. Mech. Behav. Biomed. Mater. 31, 86–99.

Rowell, S., Reyes, C., Malchau, H., Muratoglu, O., 2014. Comparative oxidative stability of highly cross-linked UHMWPE after in vivo service. Bone Jt. J. Orthop. Proc. Suppl 96, S201.

Rull, F., Prieto, A., Casado, J., Sobron, F., Edwards, H., 1993. Estimation of crystallinity in polyethylene by Raman spectroscopy. J. Raman Spectrosc. 24, 545–550.

Schmalzried, T.P., Callaghan, J.J., 1999. Current concepts review-wear in total hip and knee replacements*. J Bone Jt. Surg. 81, 115–136.

Shibata, N., Kurtz, S.M., Tomita, N., 2006. Recent advances of mechanical performance and oxidation stability in ultrahigh molecular weight polyethylene for total joint replacement: highly crosslinked and. ALPHA.-tocopherol doped. J. Biomech. Sci. Eng. 1, 107–123.

Standard, A., 2006. F2102-06, 2006. Standard guide for evaluating the extent of oxidation in ultra-high-molecular-weight polyethylene fabricated forms intended for surgical implants.

Standard, A. 2008. F2003-02, 2008. Standard practice for accelerated aging of ultra-high molecular weight polyethylene after gamma irradiation in air.

Strobl, G., Hagedorn, W., 1978. Raman spectroscopic method for determining the crystallinity of polyethylene. J. Polym. Sci.: Polym. Phys. Ed. 16, 1181–1193.

Teramura, S., Sakoda, H., Terao, T., Endo, M.M., Fujiwara, K., Tomita, N., 2008. Reduction of wear volume from ultrahigh molecular weight polyethylene knee components by the addition of vitamin E. J. Orthop. Res. 26, 460–464.

Thomas, G.E., Simpson, D.J., Mehmood, S., Taylor, A., McLardy-Smith, P., Gill, H.S., Murray, D.W., Glyn-Jones, S., 2011. The seven-year wear of highly cross-linked polyethylene in total hip arthroplasty. J. Bone Jt. Surg. 93, 716–722.

Wang, A., Sun, D., Yau, S.-S., Edwards, B., Sokol, M., Essner, A., Polineni, V., Stark, C., Dumbleton, J., 1997. Orientation softening in the deformation and wear of ultra-high molecular weight polyethylene. Wear 203, 230–241.

Yeom, B., Yu, Y.J., McKellop, H., Salovey, R., 1998. Profile of oxidation in irradiated polyethylene. J. Polym. Sci. A: Polym. Chem. 36, 329–339.

Zhu, Y., Chiu, K., Tang, W., 2001. Review article: polyethylene wear and osteolysis in total hip arthroplasty. J. orthop. Surg. 9.